

Water property monitoring and assessment for China's inland Lake Taihu from MODIS-Aqua measurements

By Wang M, W Shi and J Tan,

Remote Sensing of Environment 115 (2011) 841-854

Wei Wang

9 December 2011



南京信息工程大学

Nanjing University of Information Science & Technology

Outline

- Background
- Methods
- Results
- Discussion



1. Background

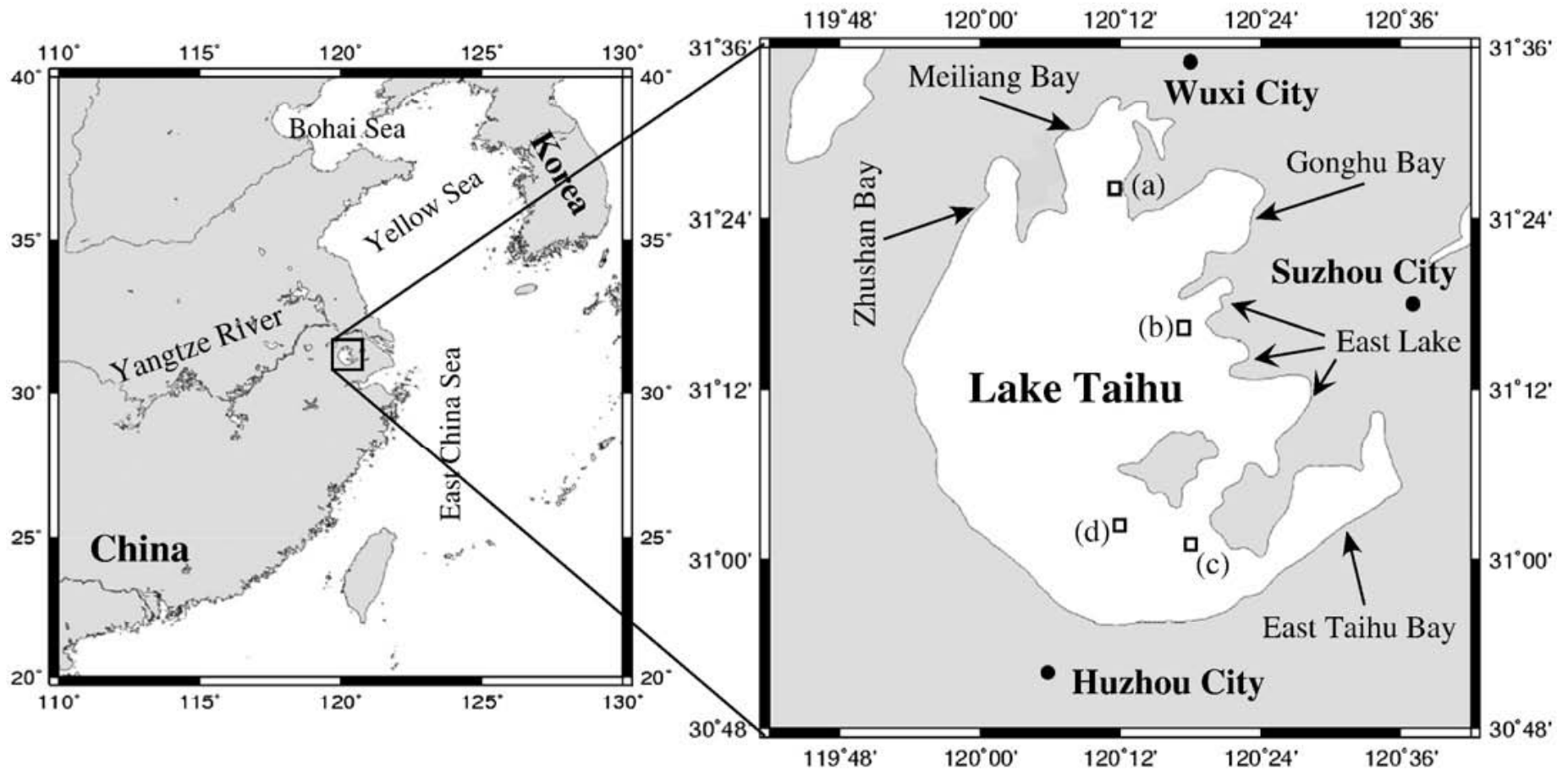


Fig. 1 Geo-location of Lake Taihu

Wang, 2011



南京信息工程大学
Nanjing University of Information Science & Technology

1.1 Why do we focus on water property in Taihu?

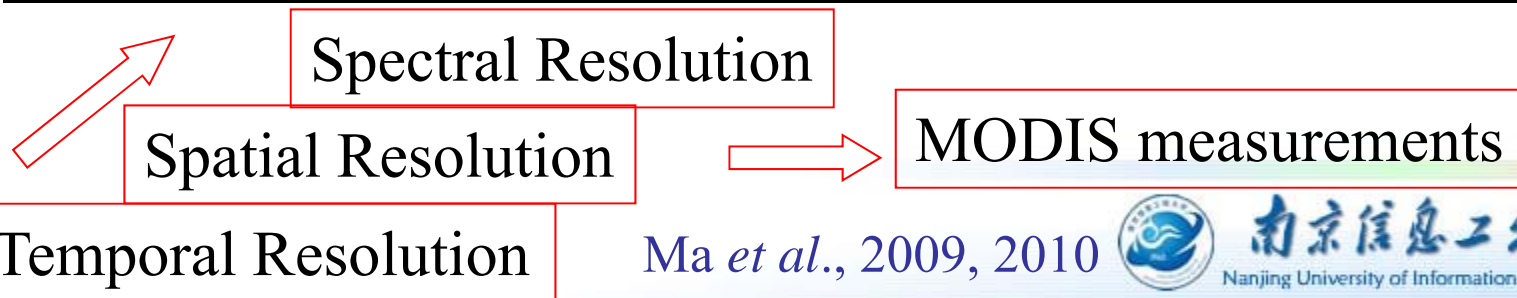
- Taihu locates in one of the world's most heavily populated regions with the rapidest economic growth.
- It helps irrigate millions of ha. of farmlands, also provides drinking water for more than 2 million people, and sustains one of China's most important fisheries (Guo, 2007) .
- Since 1980s, Taihu has become more and more eutrophic. In early June 2007, massive blue-green algae bloomed over Taihu, contaminating tap water for millions of Wuxi residents (Ding, *et al.*, 2007; Hu *et al.*, 2010).





Table 1 Comparison between Remote Sensing (RS) and In situ measurement

	Remote Sensing	In situ measurement
Temporal coverage	High rate, long-term	Low rate, short-term
Spatial coverage	Broad field of view	Fixed locations
Characteristics	Rapid, synoptic, repeated, stable	Labor-intensive, confined to short period, restricted by external conditions



Ma *et al.*, 2009, 2010



南京信息工程大学
Nanjing University of Information Science & Technology

1.2 Basic knowledge for Lake Color RS

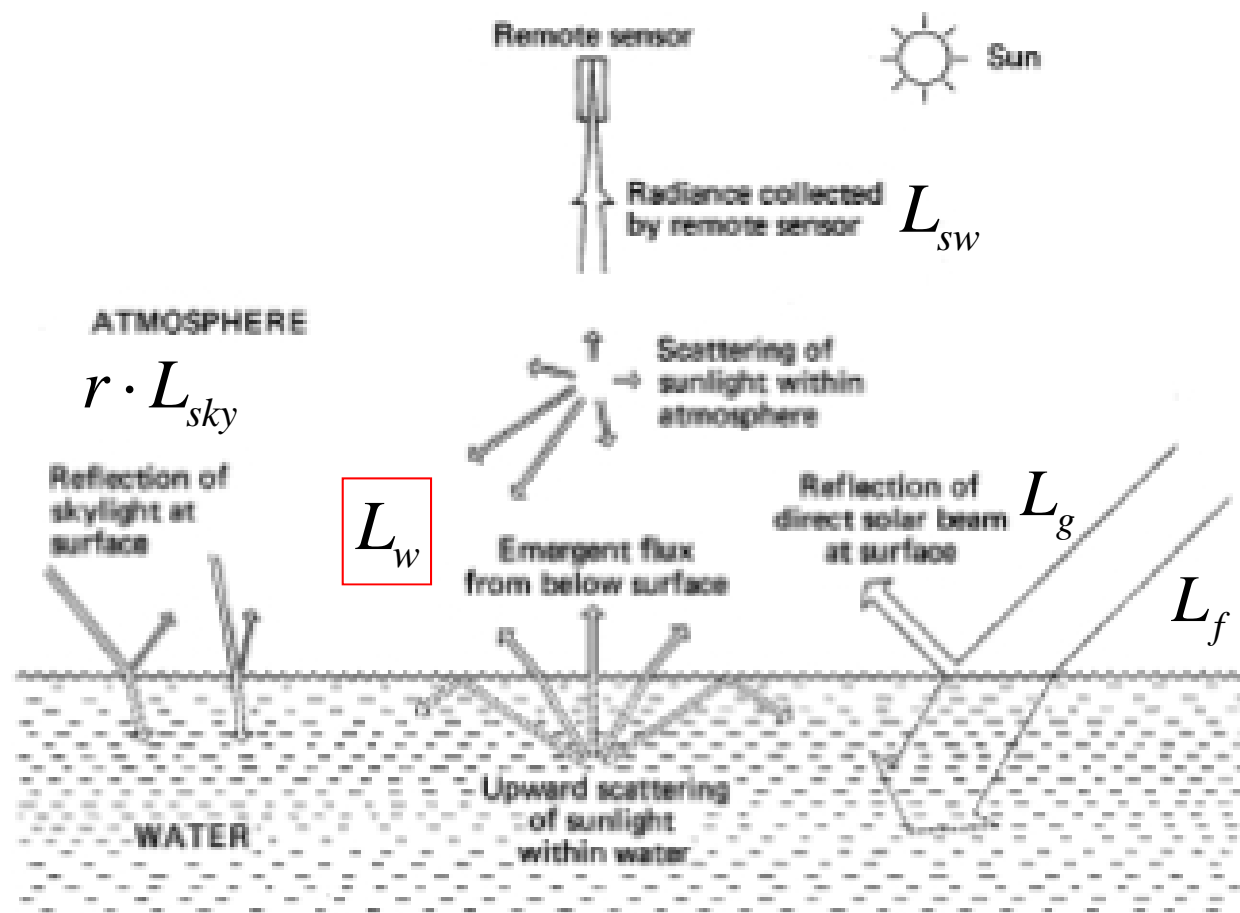


Fig. 1 Above water signal composition (Kirk, 2011)



$$L_{sw} = L_w + r \cdot L_{sky} + L_f + L_g$$

$$nL_w(\lambda) = L_w \cdot \frac{F_0}{E_d(0^+)} \quad \text{Ma et al., 2010}$$

L_{sw} Radiance received by sensors L_w Water-leaving radiance

r Reflectivity of water-atmosphere interface L_{sky} Skylight radiance

L_f Radiance contributions of white cap L_g Sunlint specular

nL_w Normalized water-leaving radiance $E_d(0^+)$ Incident radiance above surface

F_0 Top of atmosphere radiance at mean Earth-Sun distance

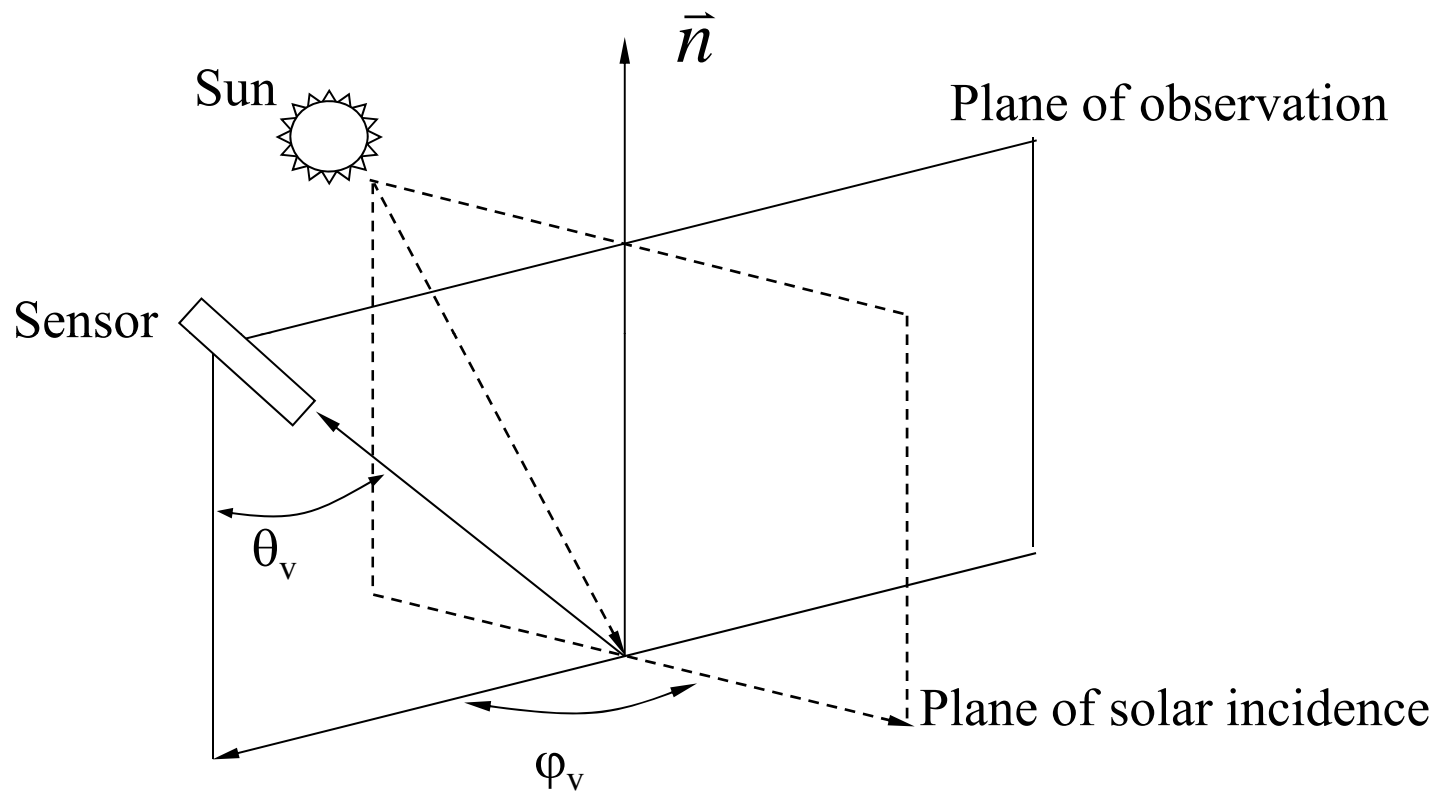


Fig. 2 Viewing geometry of above-water measurement (Tang *et al.*, 2004)



Table 2 Optical properties of Lake water (Case II Waters) (Ma *et al.*, 2010)

Apparent optical properties (AOPs)	Water leaving radiance
	Normalized water-leaving radiance
	Reflectance
	Remote sensing reflectance
	Diffuse attenuation coefficient of water
	Diffuse attenuation coefficient of irradiance
Inherent optical properties (IOPs)	Absorption coefficient
	Scattering coefficient
	Scattering phase function
	Volume scattering coefficient
	Beam attenuation coefficient

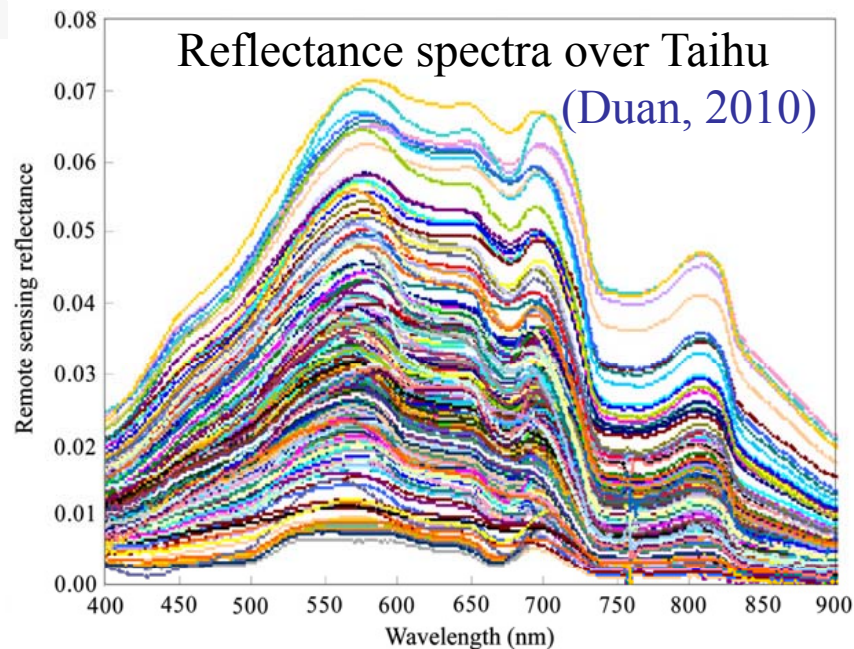
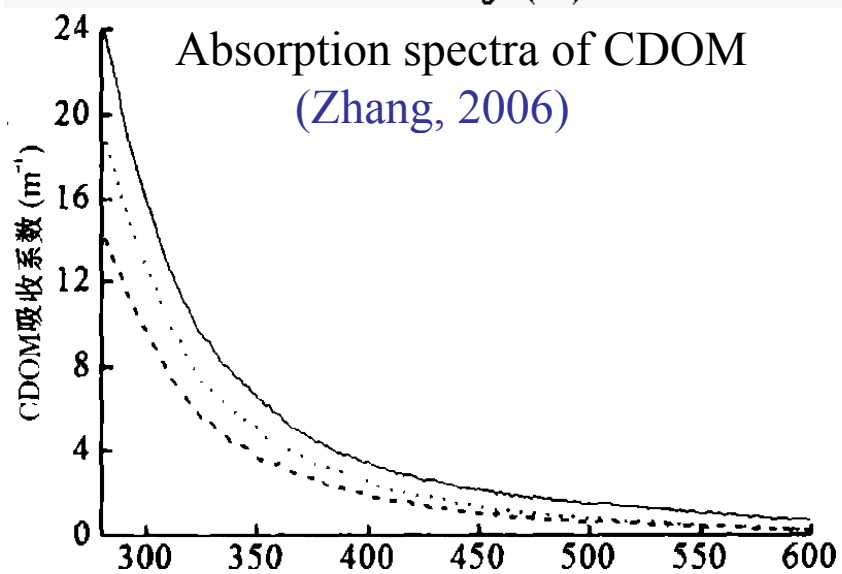
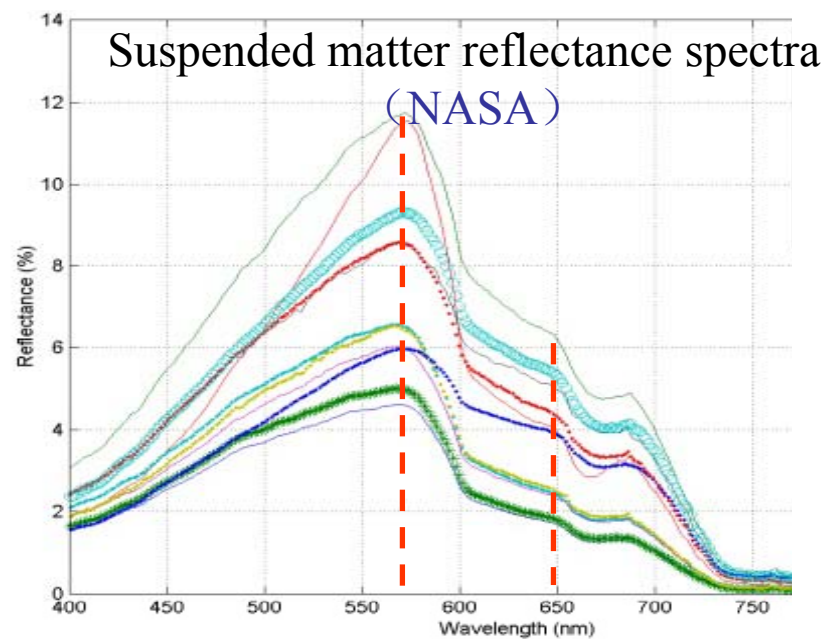
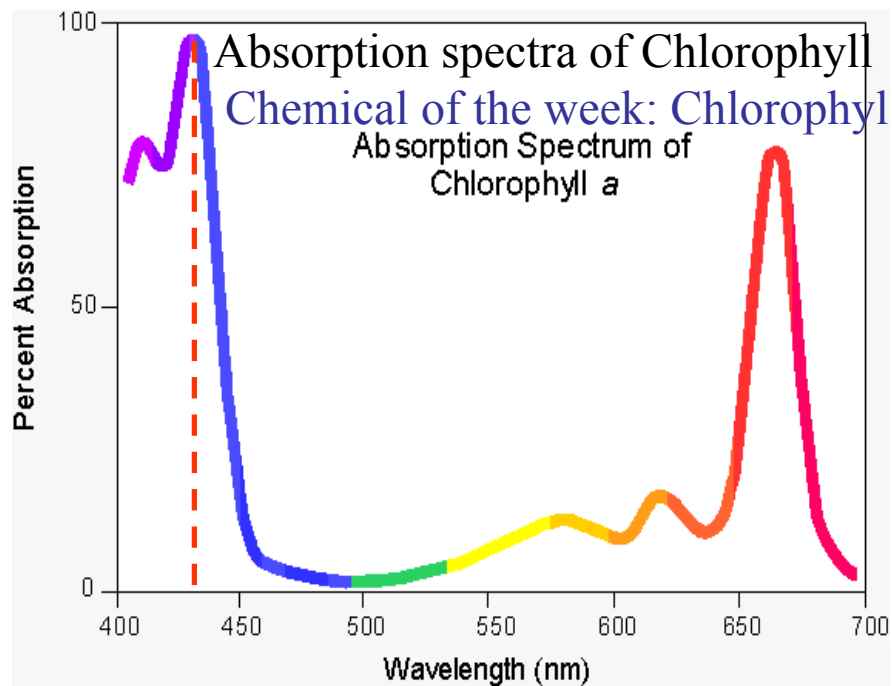


Fig.3 Typical spectral

Table 3 Atmospheric correction algorithm suitable for Water Color RS (Ma *et al.*, 2010)

	Ocean Color RS	Lake Color RS
Characteristic	$L_{w, near-infrared} = 0$	$L_{w, near-infrared} \neq 0$
Algorithm	Gordon algorithm for CZCS (Gordon, 1993)	Principal component analysis (Neumann, 1995)
	Gordon algorithm for SeaWiFs (Gordon and Wang, 1994)	Arnone iteration (Arone, 1998)
	Gordon algorithm for MODIS (Gordon and Voss, 1999)	Artificial neural network method (Doerffer and Schiller, 1998)
		Absorption coefficient iteration in near infrared (Aiken and Moore, 2000)
		Hu algorithm (Hu, 2000)
		Ruddick algorithm (Ruddick, 2000, 2001)
		Fixed remote sensing reflectance algorithm (He and Pan, 2003)
	Shortwave infrared (SWIR) algorithm (Wang and Shi, 2005)	

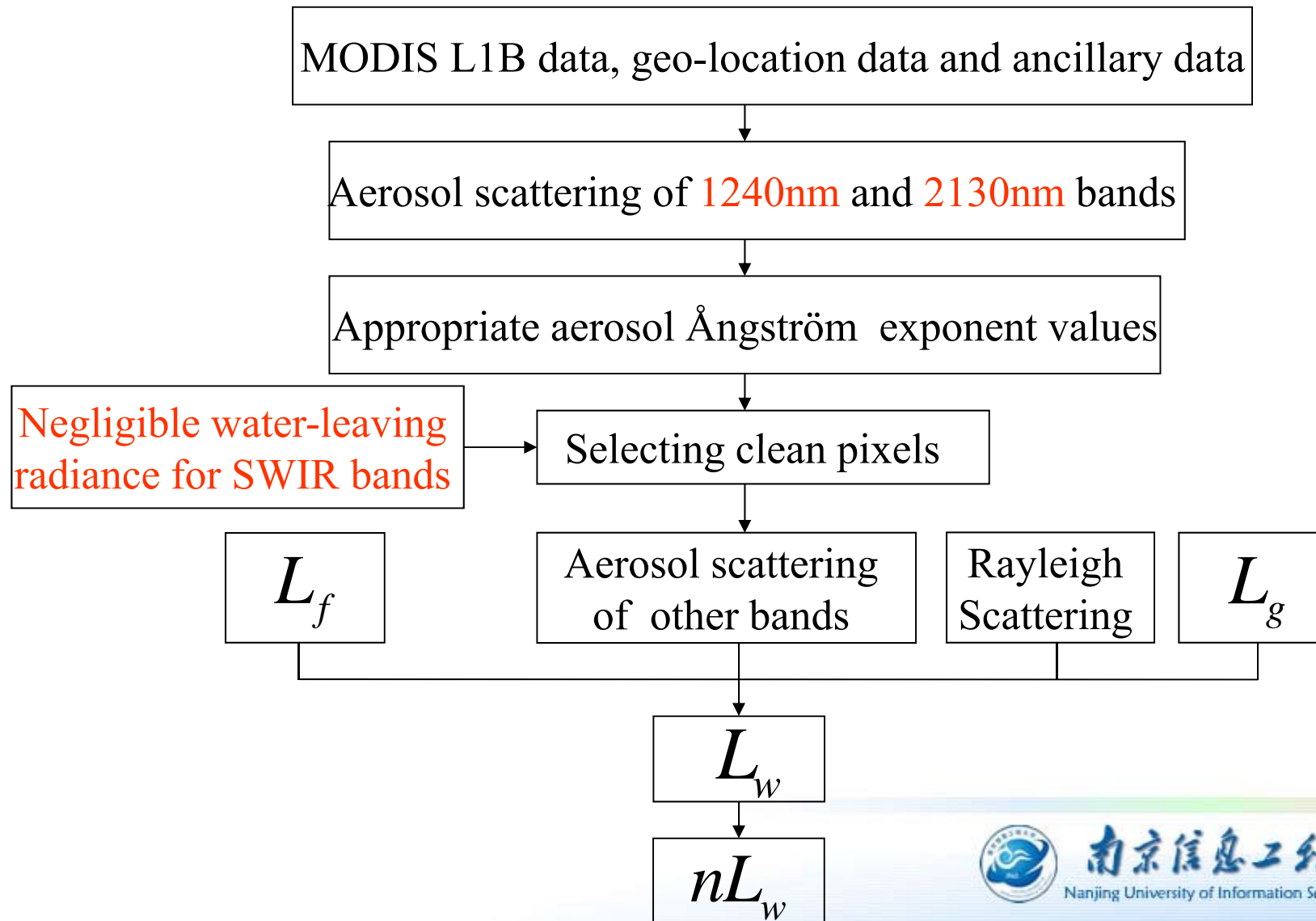
2. Methods

Table 4 Data set

In situ data	Water-leaving radiance spectral (10-18 June 2007) a (31.43° N, 120.20° E), b (31.27° N, 120.29° E) c (31.95° N, 120.31° E), d (31.06° N, 120.19° E)
MODIS-Aqua images	2002-2008 29 March, 19 April, 7 May, 14 May, 8 June 2007
Validation data (From CERN)	In situ Chl-a concentration 17 March (13), 15 April (13), 15-18 May (31), 15 June (13) 2007



Fig. 4 Flow chart of SWIR-based atmospheric correction algorithm



Deriving Chl-a concentration and diffuse attenuation coefficient $K_d(490)$ from nL_w spectra

$$C_a = 10.0(0.366 - 3.067R_{4M} + 1.930R_{4M}^2 + 0.649R_{4M}^3 - 1.532R_{4M}^4)$$

where $R_{4M} = \log_{10}(R_{550}^{443} > R_{550}^{490} > R_{550}^{530})$ O'Reilly et al., 2000

$$K_d(490) = -0.05256 + 1.3537 \frac{R_{rs}(670)}{R_{rs}(490)},$$

for $0.3 \text{ m}^{-1} < K_d(490) < 0.6 \text{ m}^{-1}$ Wang *et al.*, 2009



南京信息工程大学

Nanjing University of Information Science & Technology

3. Results

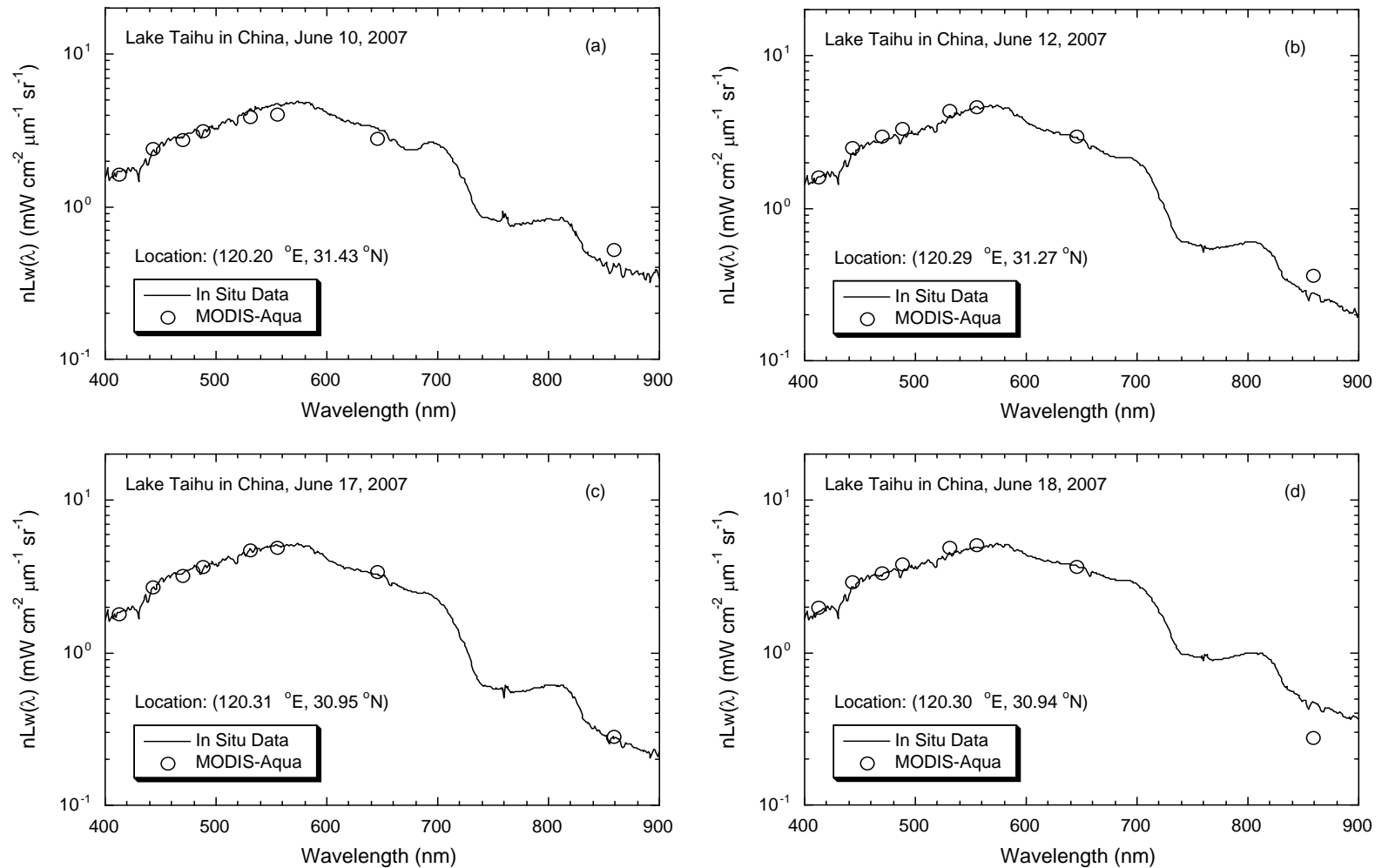
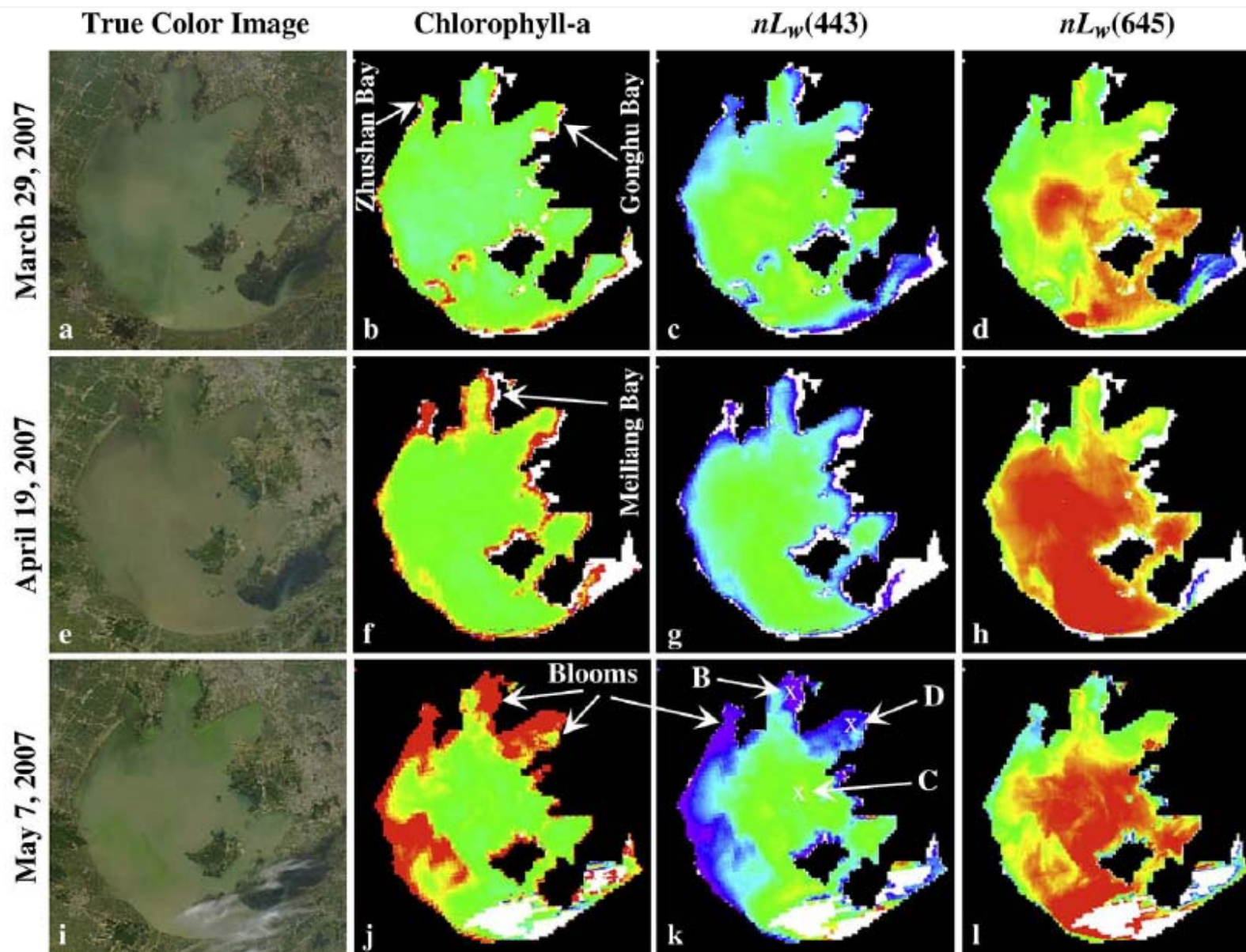


Fig.5 Comparison of normalized water-leaving radiance spectra

Importance of $nL_w(\lambda)$ for typical bands

- $nL_w(443)$: representing characteristic of algae absorption, **low** value corresponds to **high** algae concentration;
- $nL_w(555)$, $nL_w(645)$, $nL_w(859)$: representing variation of total suspended sediment (TSS), **high** value corresponds to **high** TSS concentration ;
- $K_d(490)$: water diffuse attenuation coefficient at 490nm, **low** value corresponds to **high-clarity** waters.





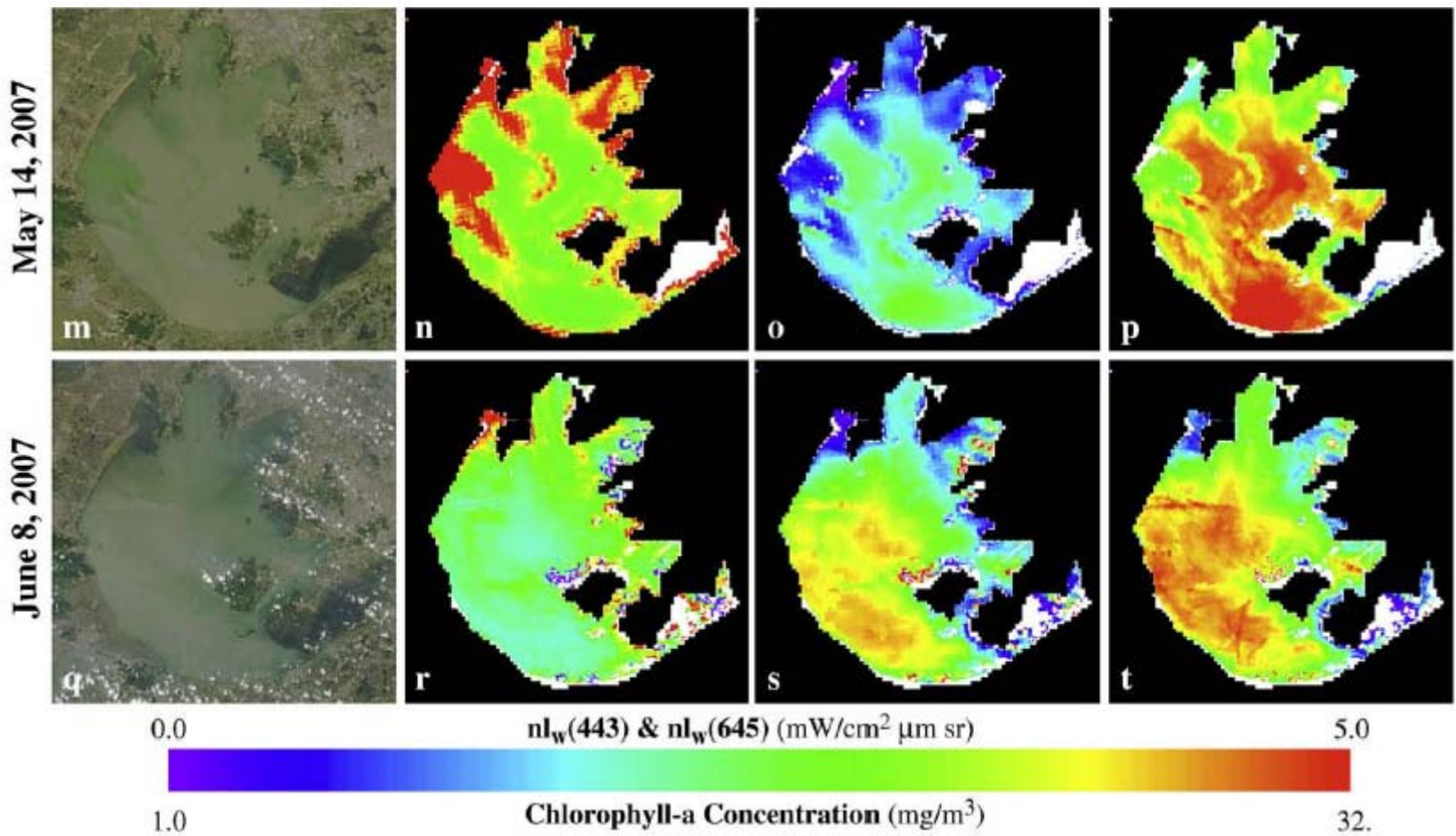


Fig.6 MODIS-Aqua monitoring for 2007 algae bloom in Taihu

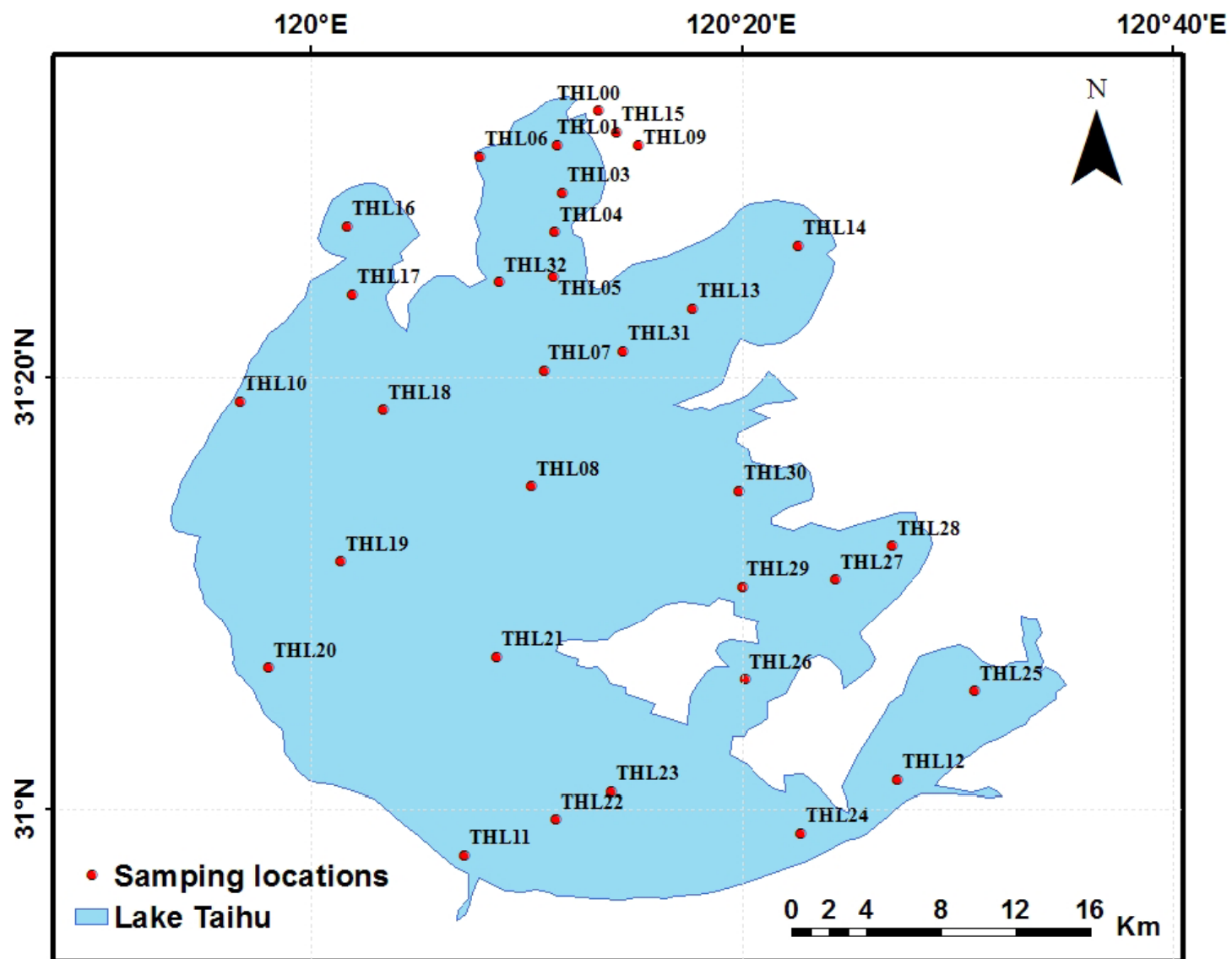


Fig.7 Sampling locations distribution in Taihu

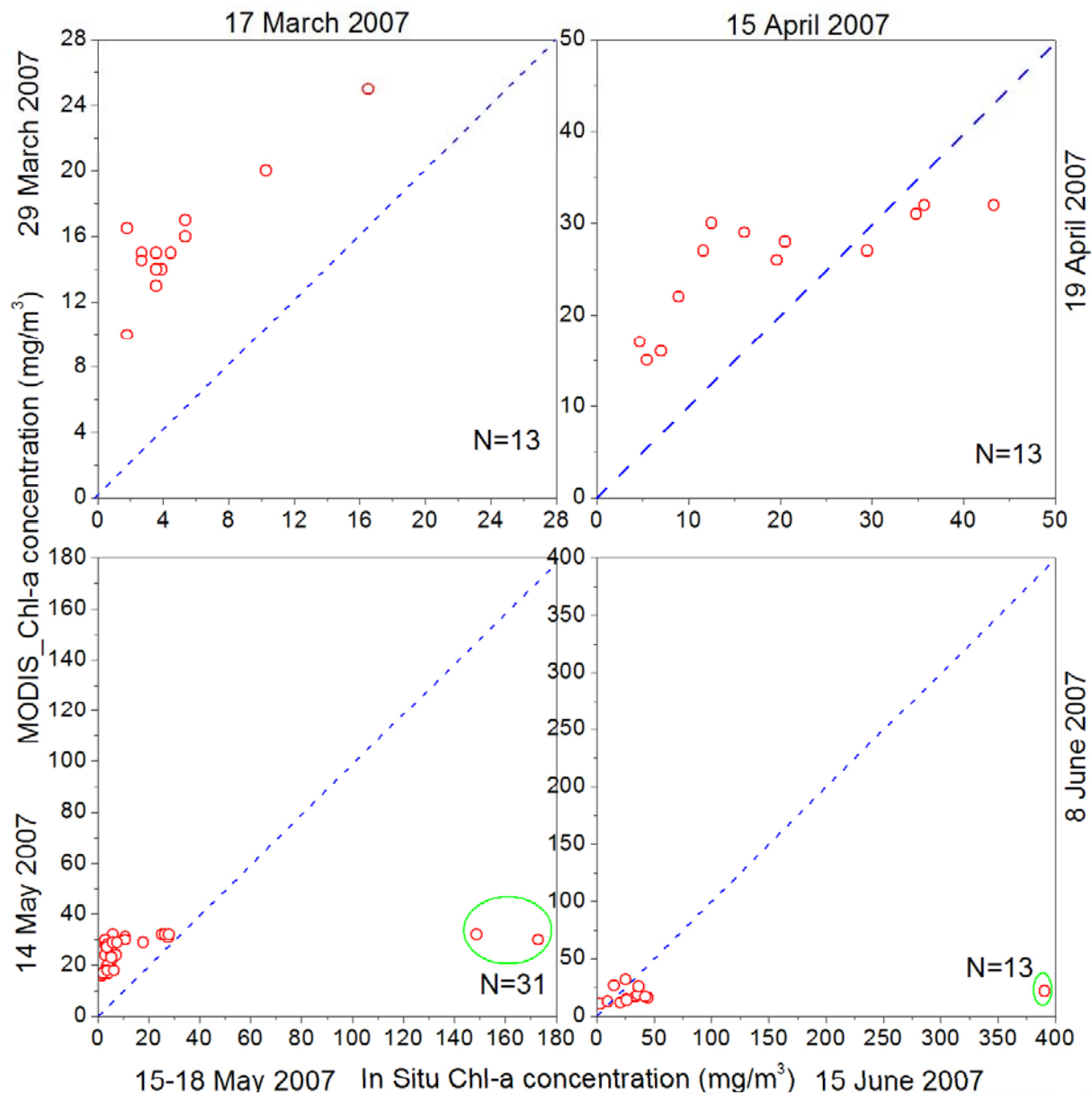
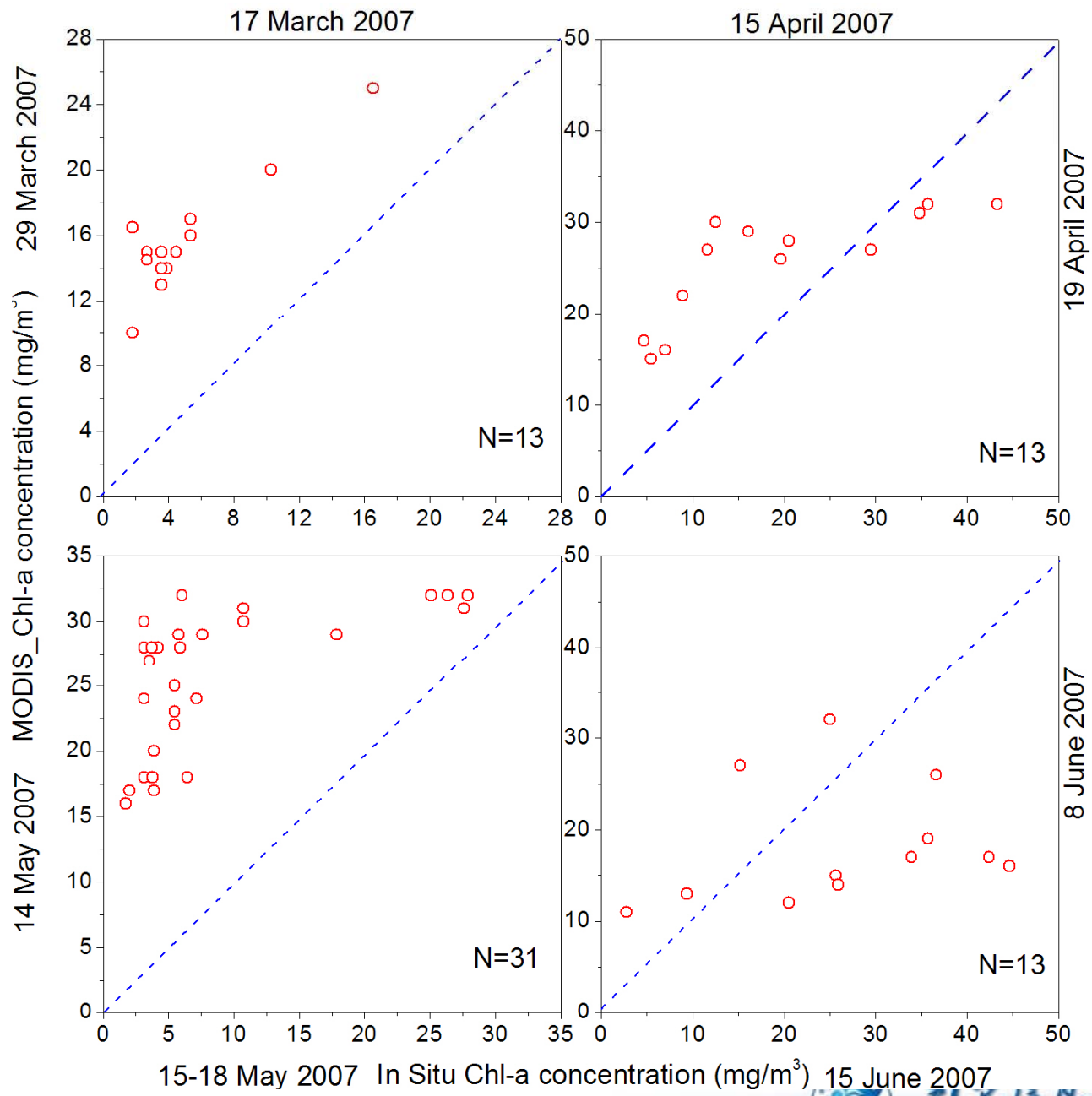


Fig.8 Chl-a concentration comparison between MODSI retrieval and in situ observation (monthly)





15-18 May 2007 In Situ Chl-a concentration (mg/m³) 15 June 2007

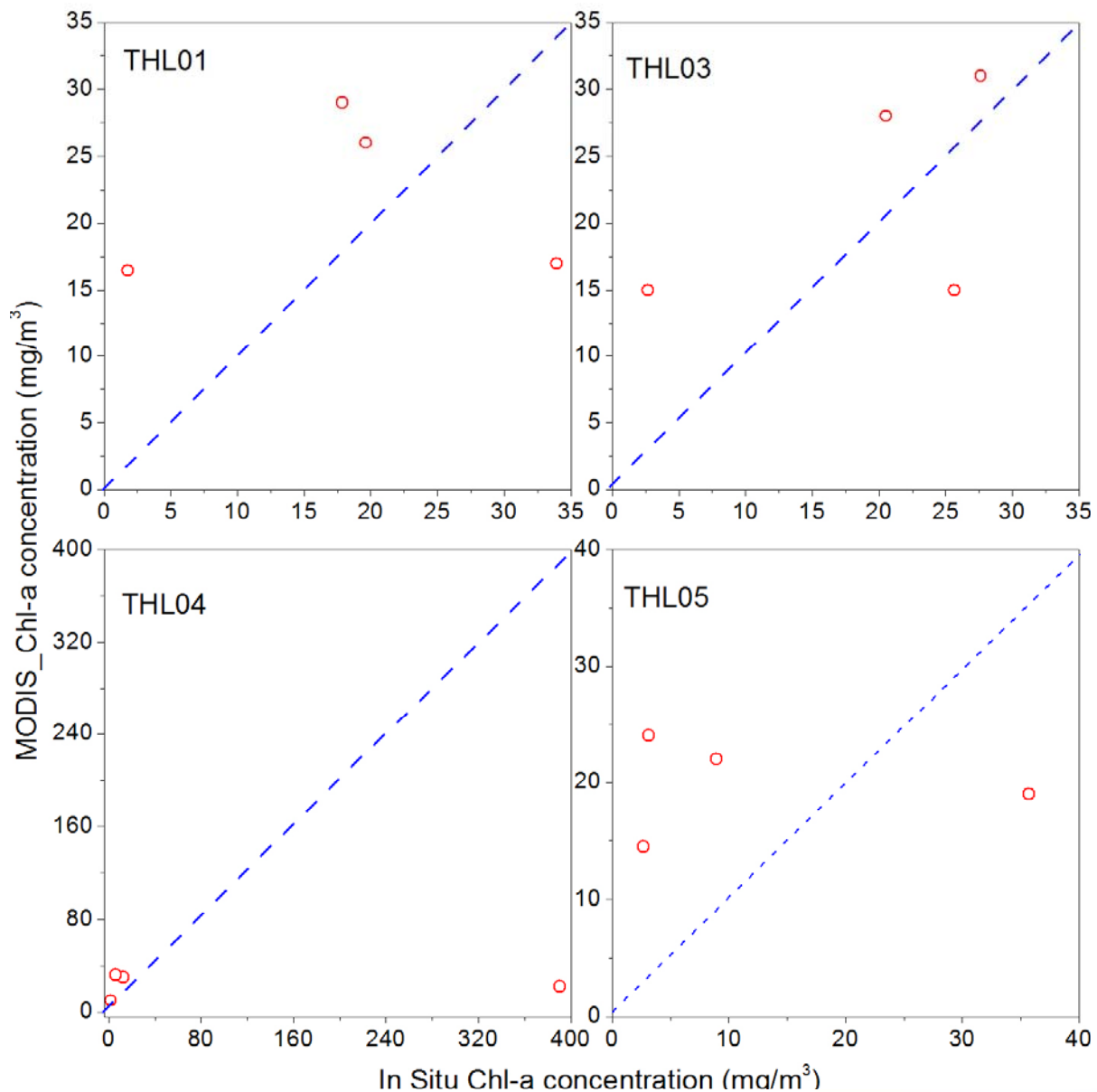
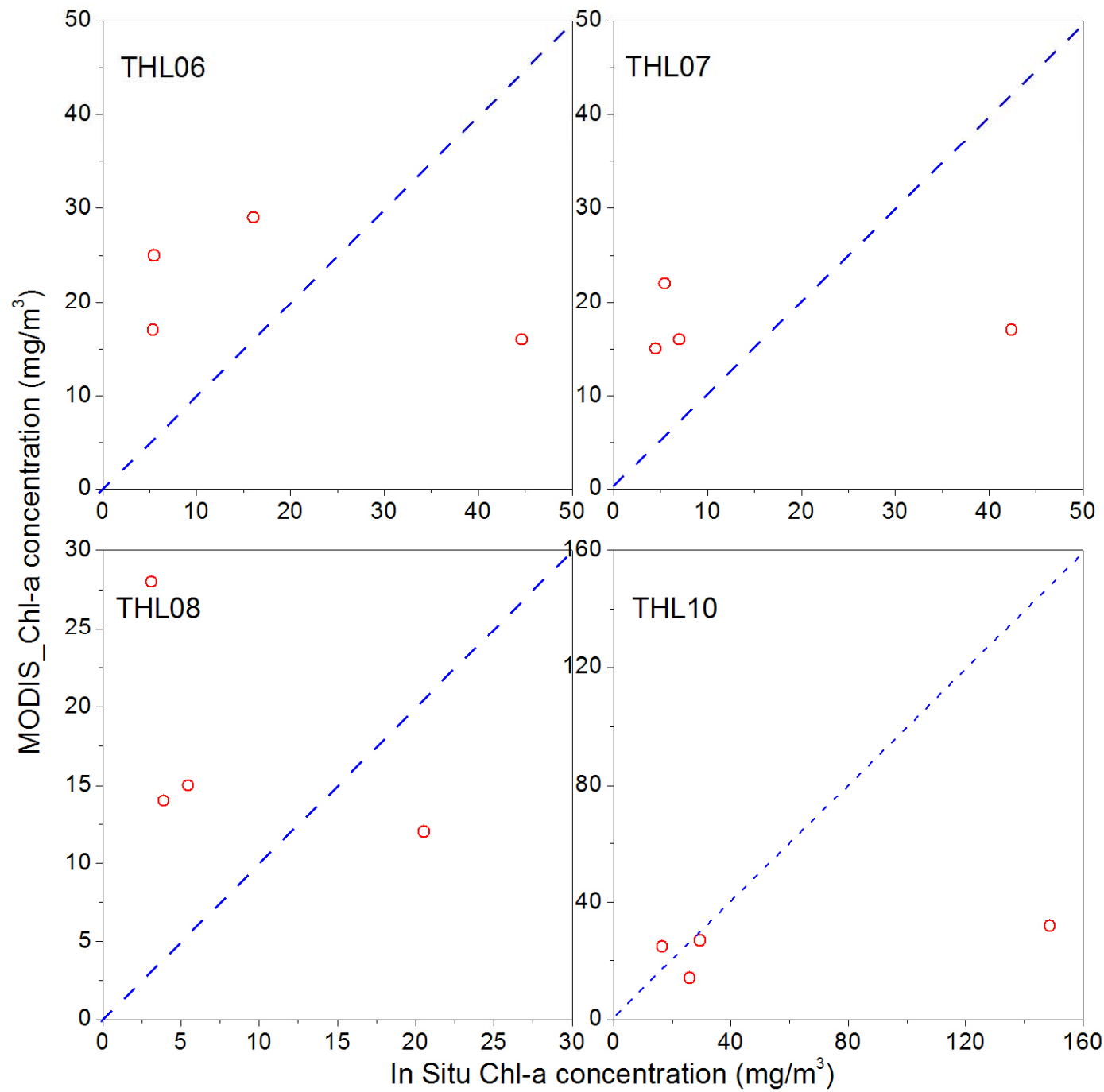
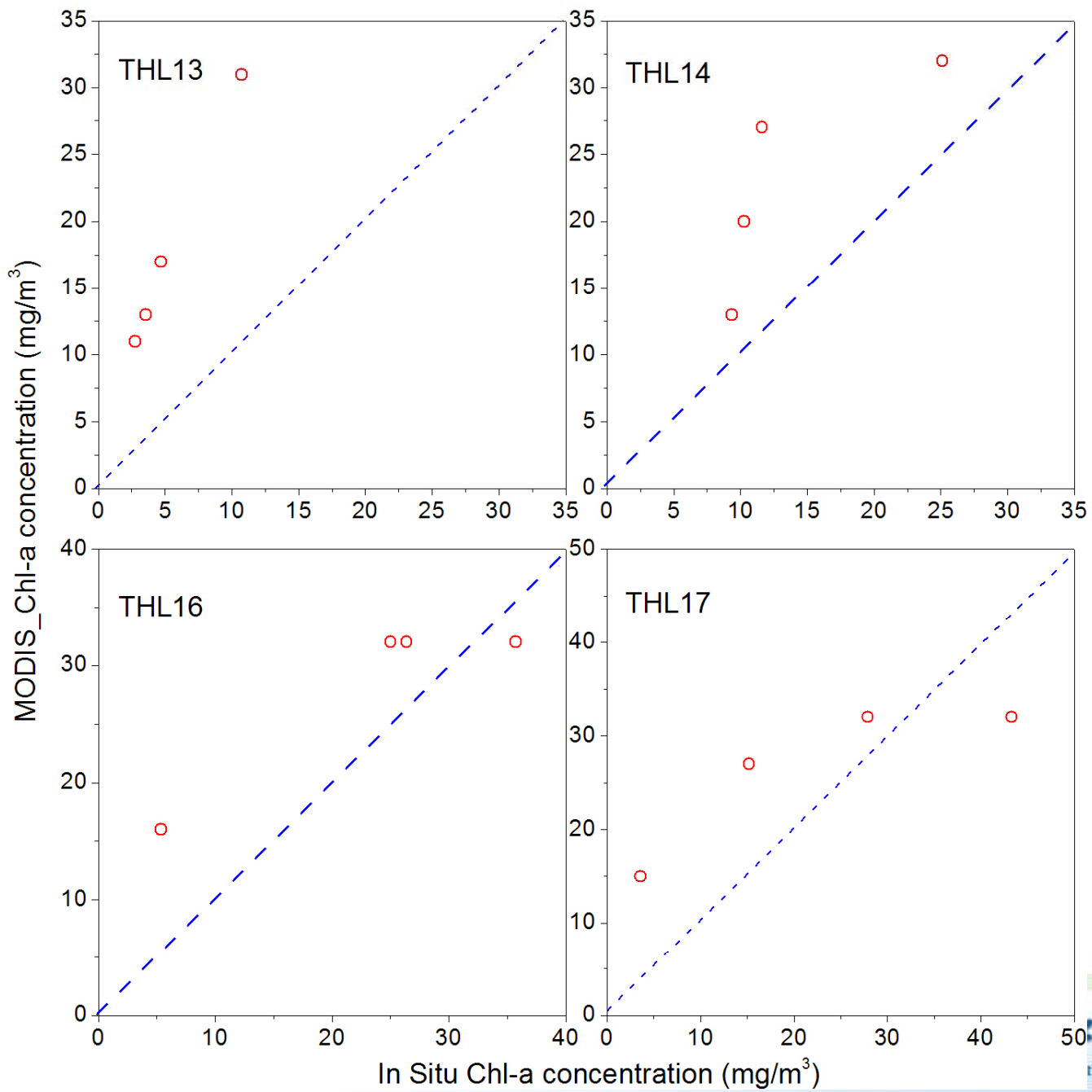
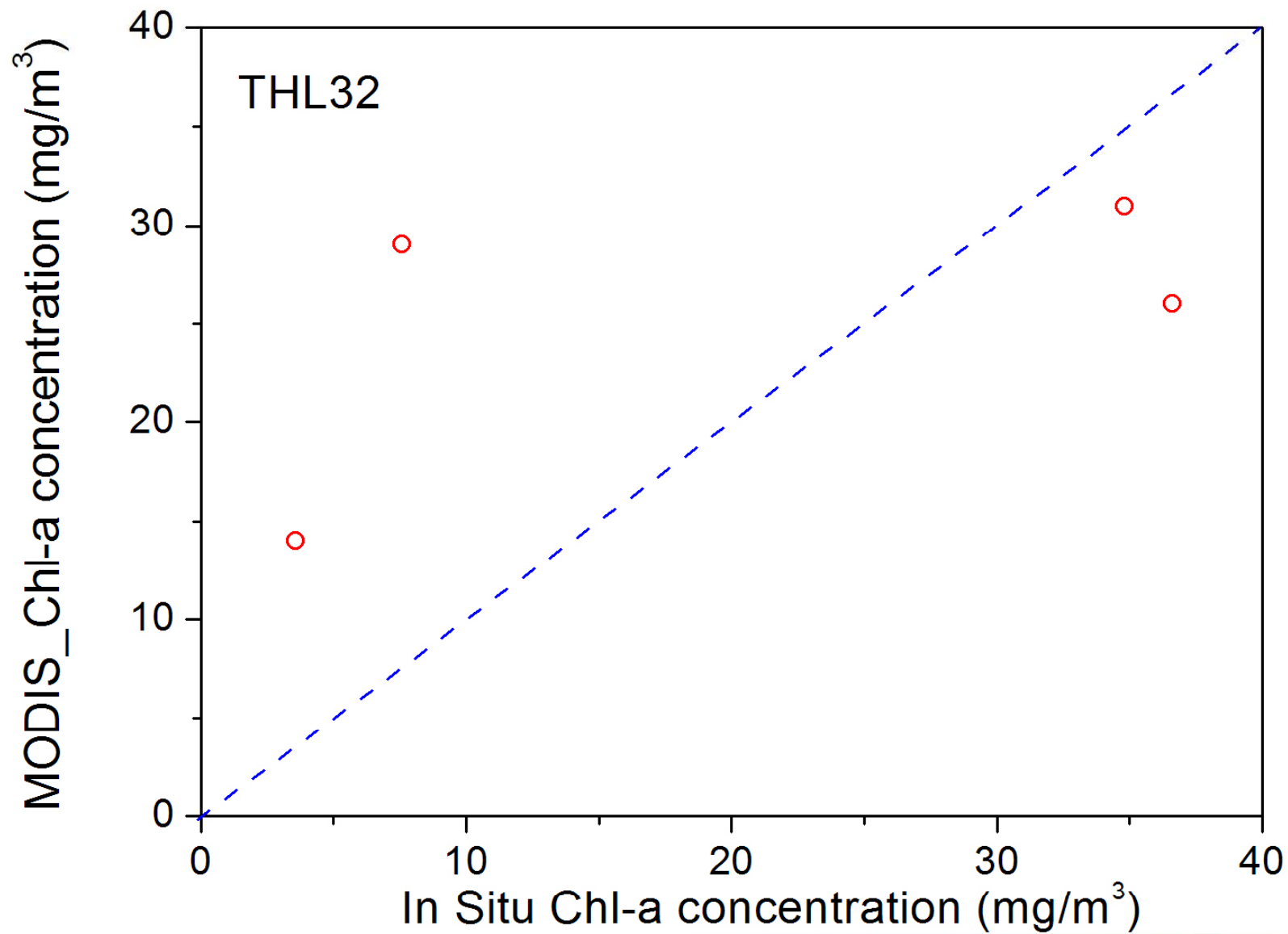


Fig.9 Chl-a concentration comparison between MODSI retrieval and in situ observation (every location)







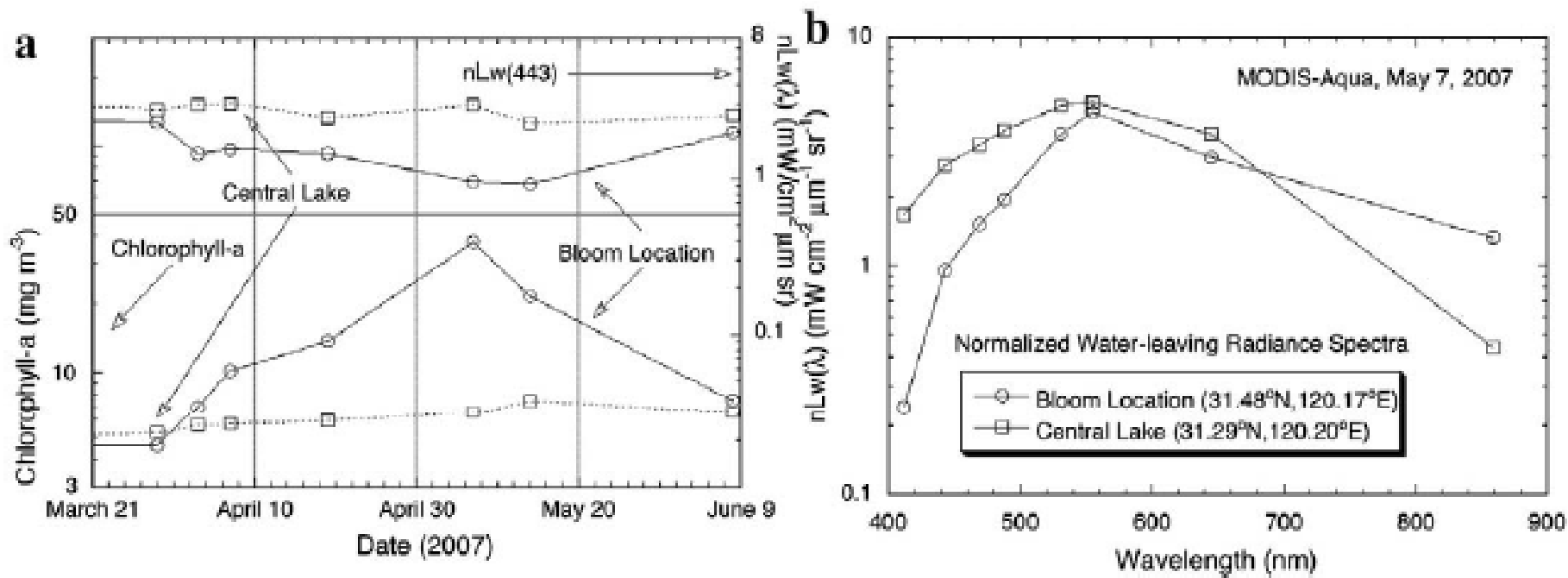


Fig. 10 (a) MODIS derived time series (29 March to 8 June 2007) for Chl-a and nL_w(443), (b) nL_w(λ) spectral on 7 May 2007 for algae contaminated and non-contaminated waters.

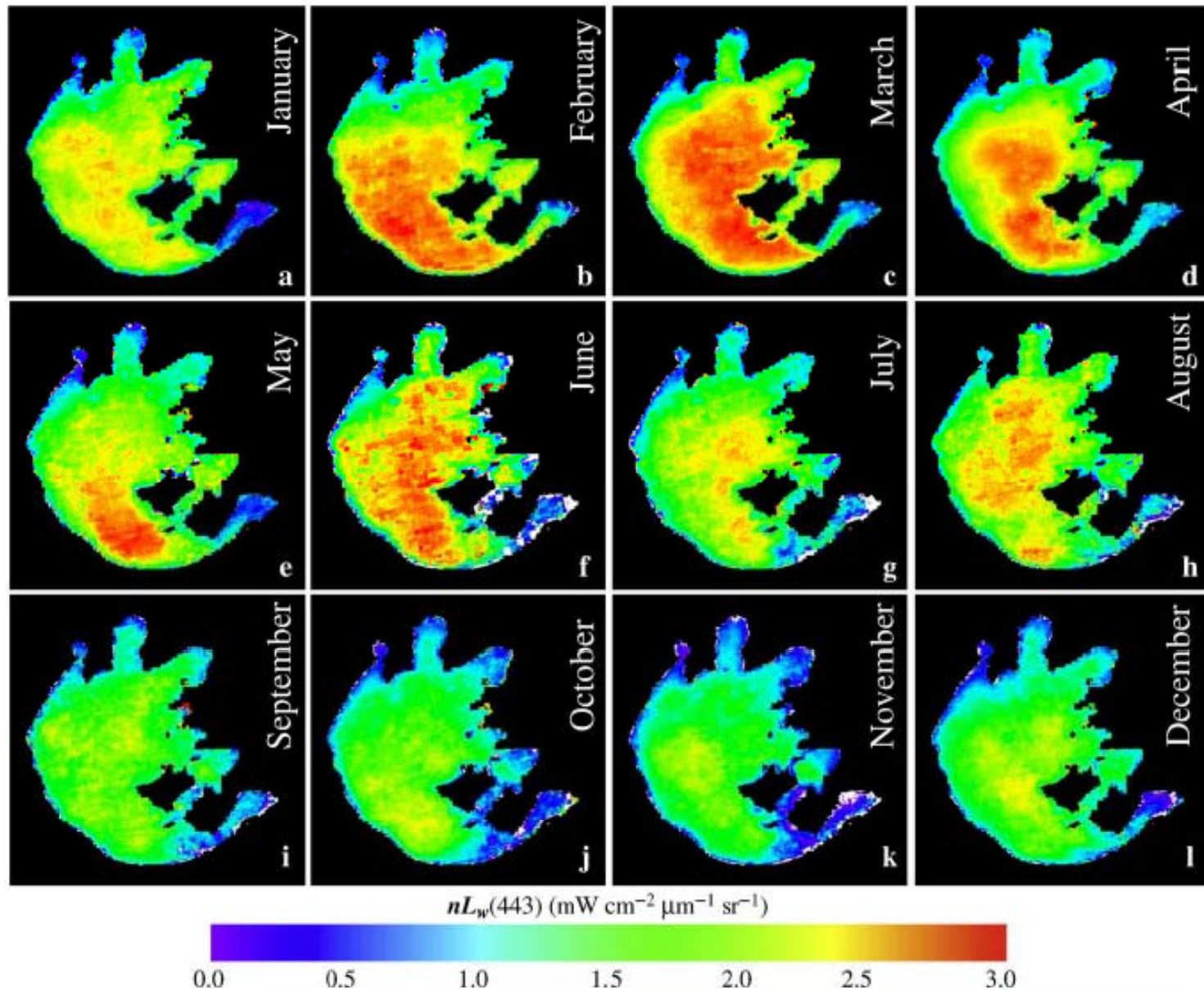
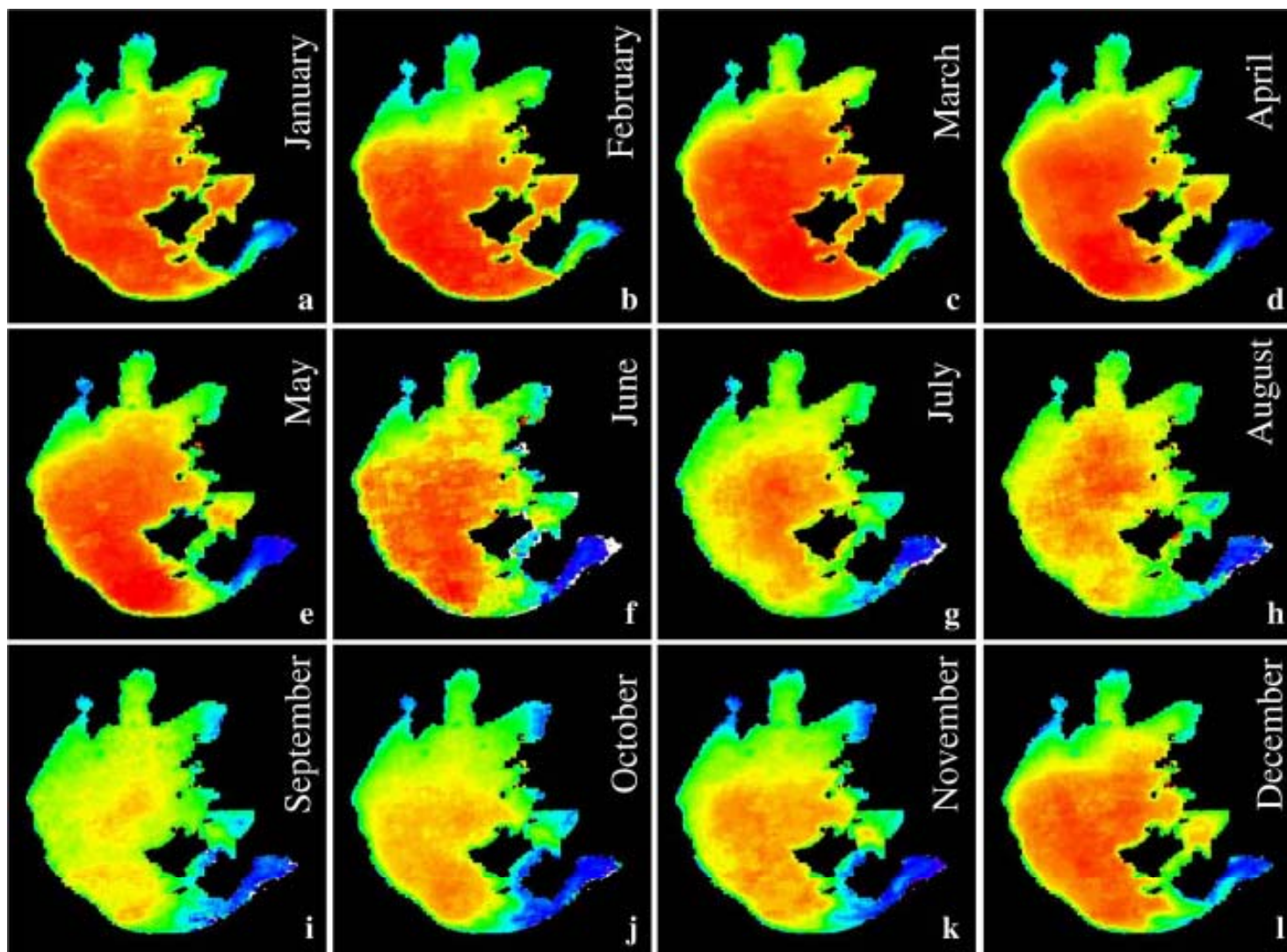


Fig. 11 MODSI-derived (2002-2008) monthly climatology $nL_w(443)$





$nL_w(555)$ ($\text{mW cm}^{-2} \mu\text{m}^{-1} \text{sr}^{-1}$)

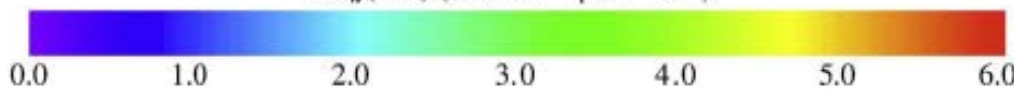


Fig. 12 MODSI-derived (2002-2008) monthly climatology $nL_w(555)$



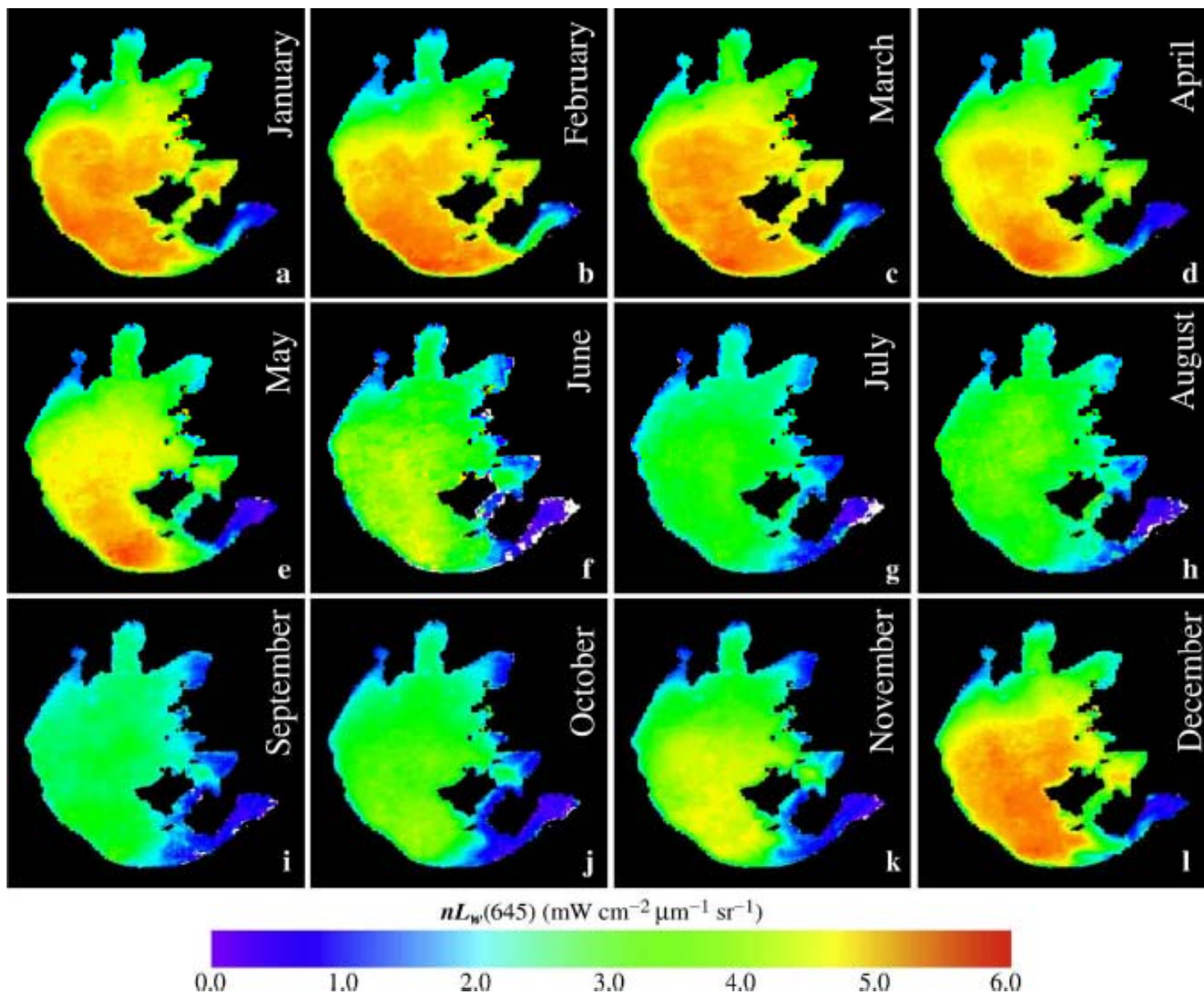
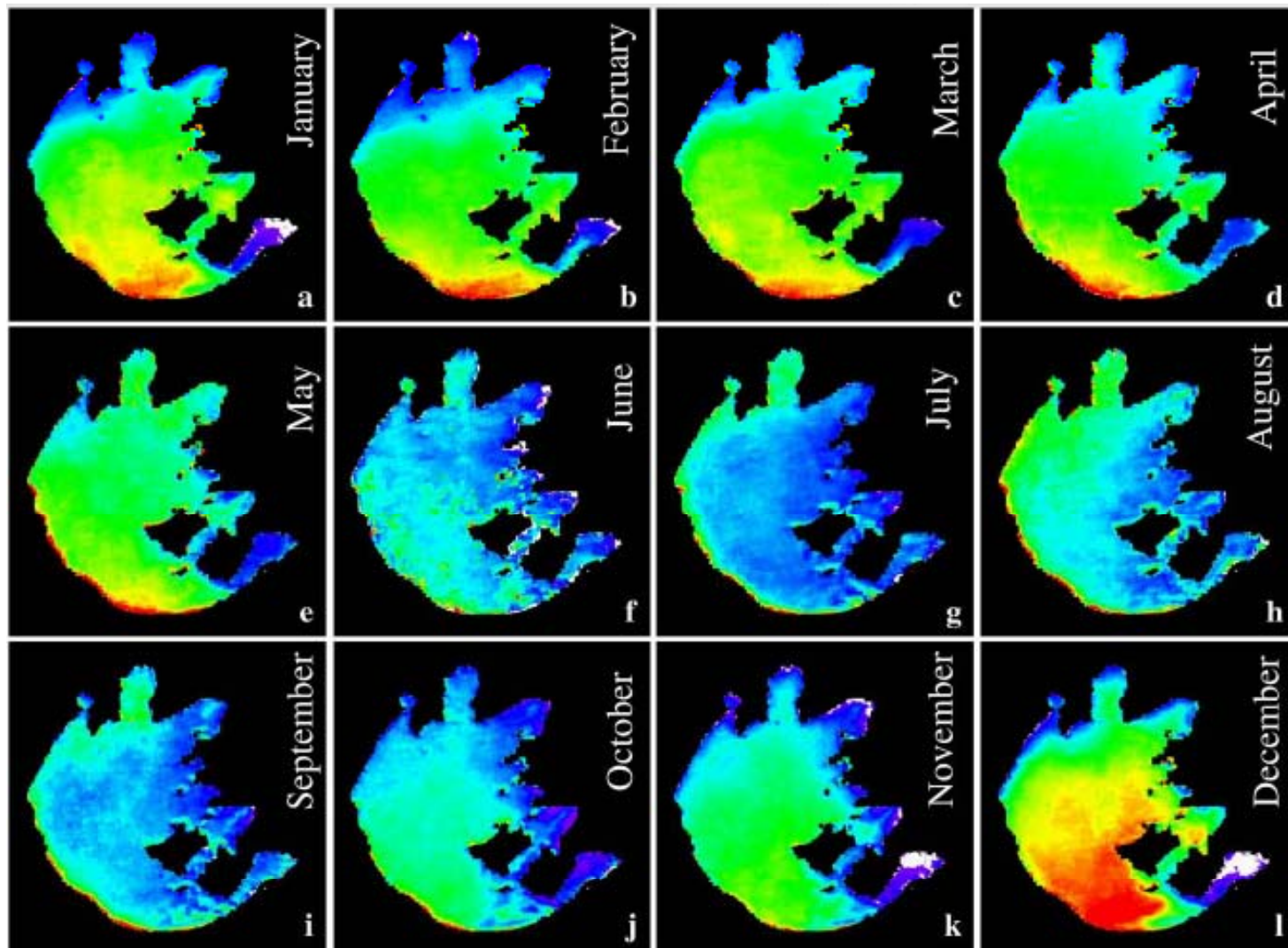


Fig. 13 MODSI-derived (2002-2008) monthly climatology $nL_w(645)$





$nL_w(859)$ ($\text{mW cm}^{-2} \mu\text{m}^{-1} \text{sr}^{-1}$)



0.0

1.0

2.0

Fig. 14 MODSI-derived (2002-2008) monthly climatology $nL_w(859)$



南京信息工程大学

Nanjing University of Information Science & Technology

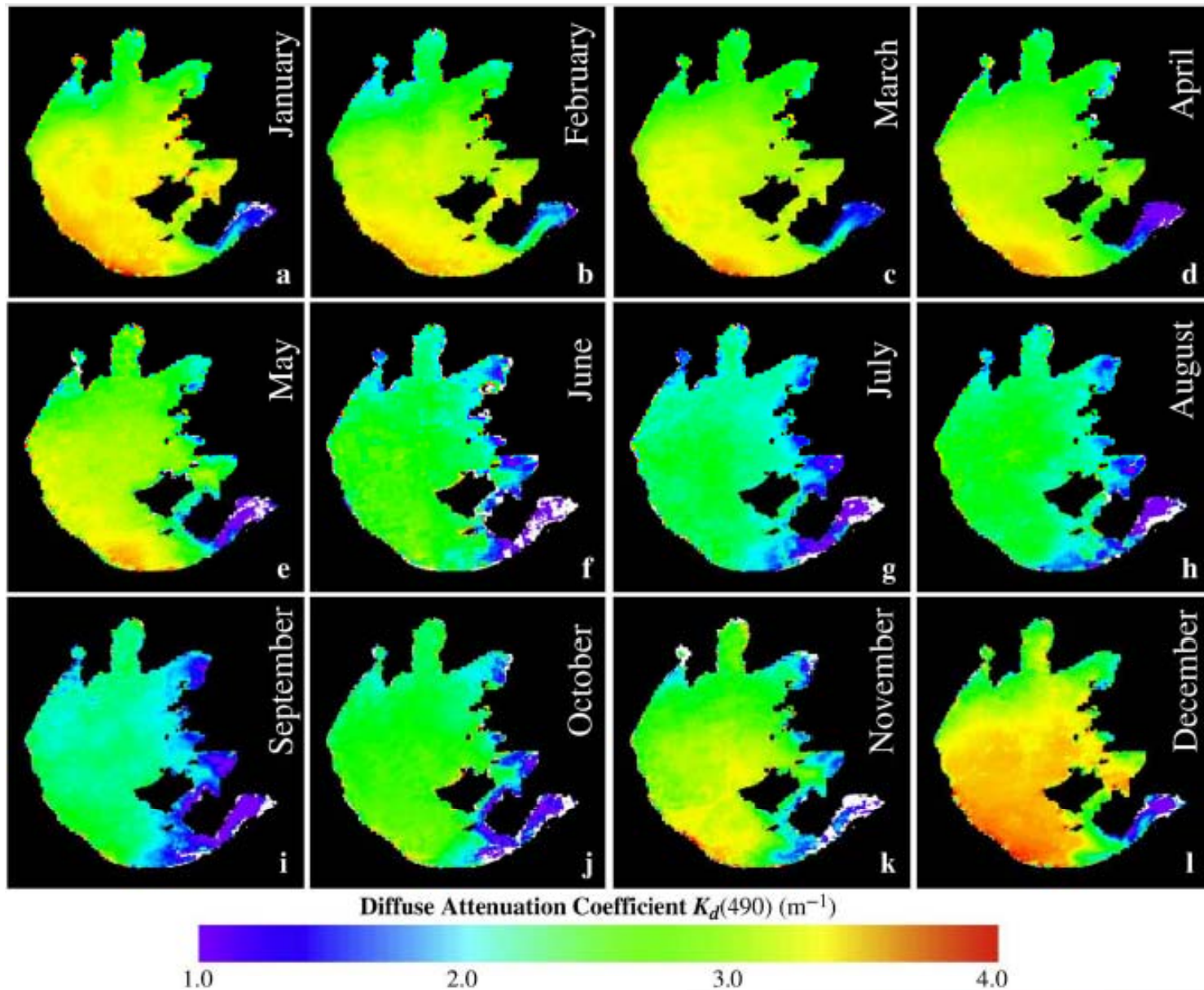


Fig. 15 MODSI-derived (2002-2008) monthly climatology $K_d(490)$



南京信息工程大学

Nanjing University of Information Science & Technology

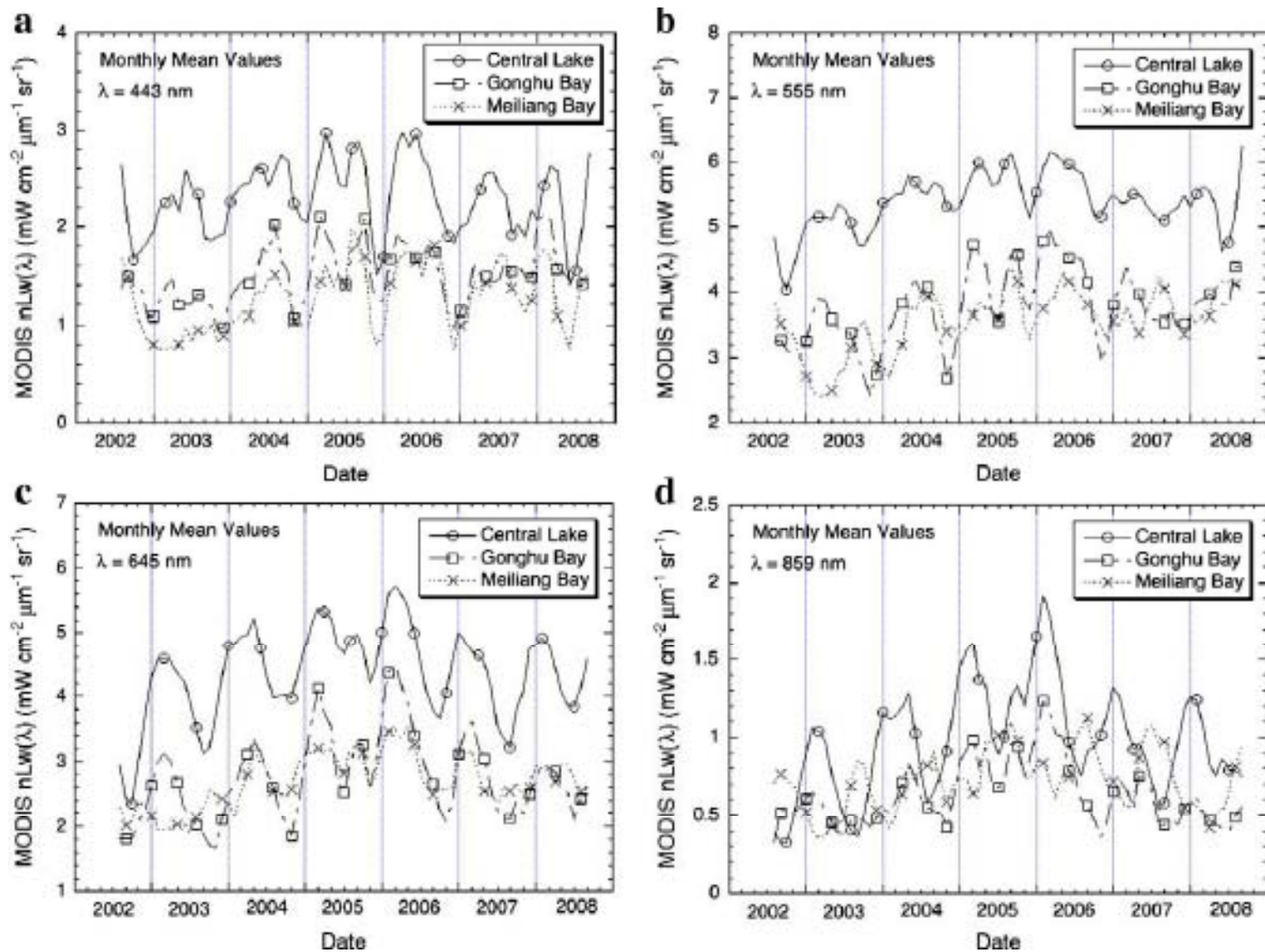


Fig. 16 MODSI-derived $K_d(490)$ for central lake, Gonghu Bay and Meiliangwan Bay

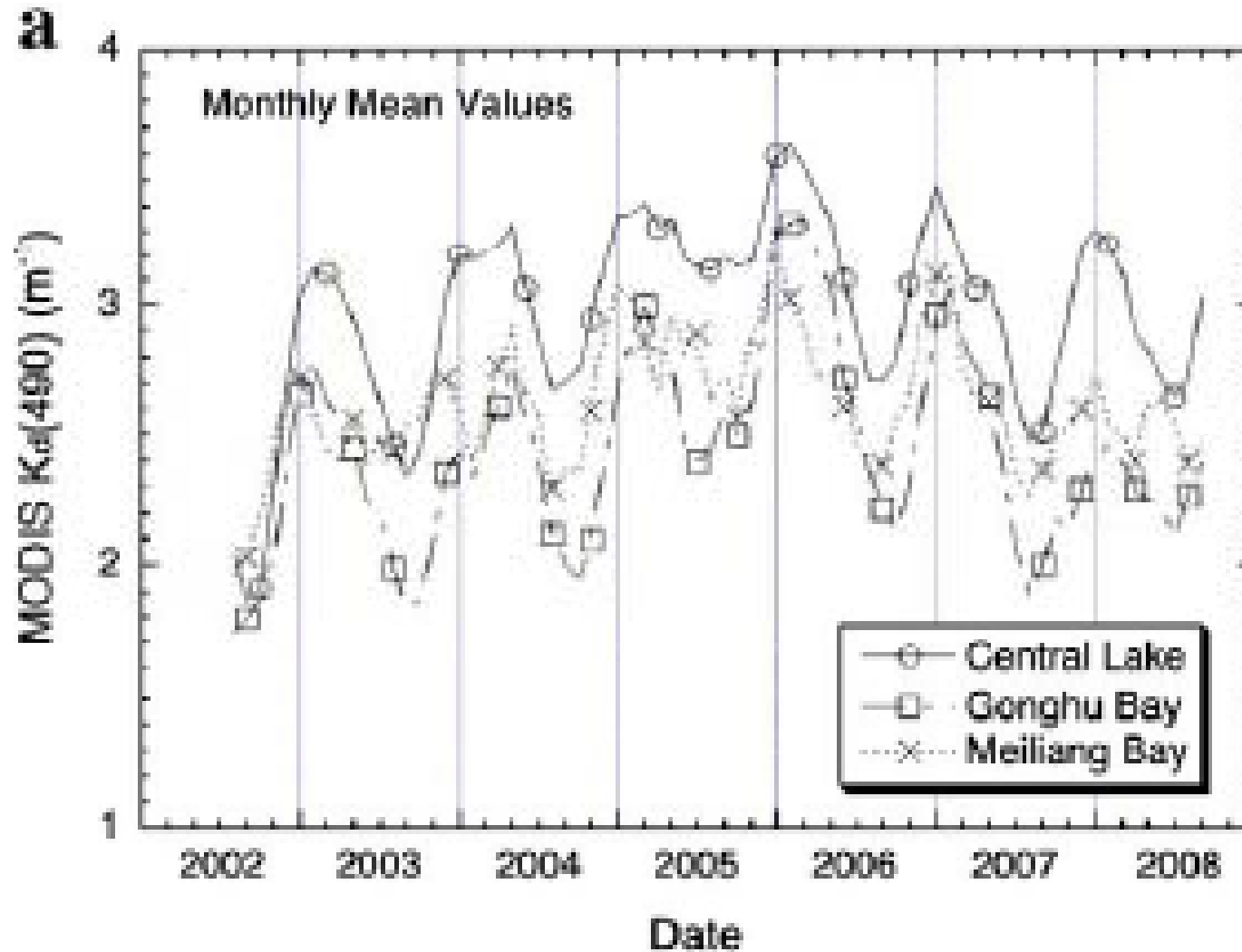


Fig. 17 Seasonal variability of MODSI-derived $K_d(490)$ for the central lake, Gonghu Bay and Meiliangwan Bay

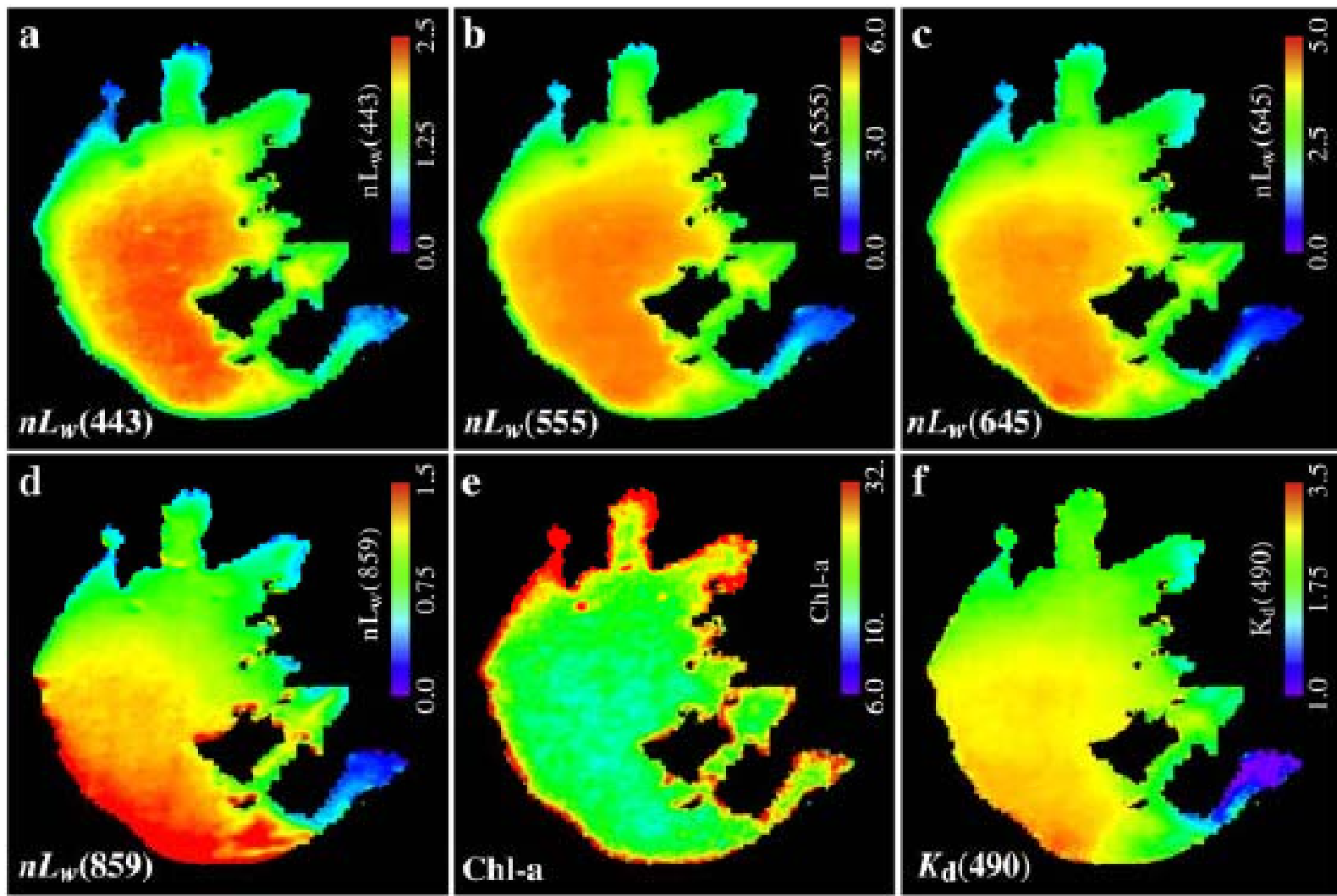


Fig. 18 MODSI-derived climatology water property



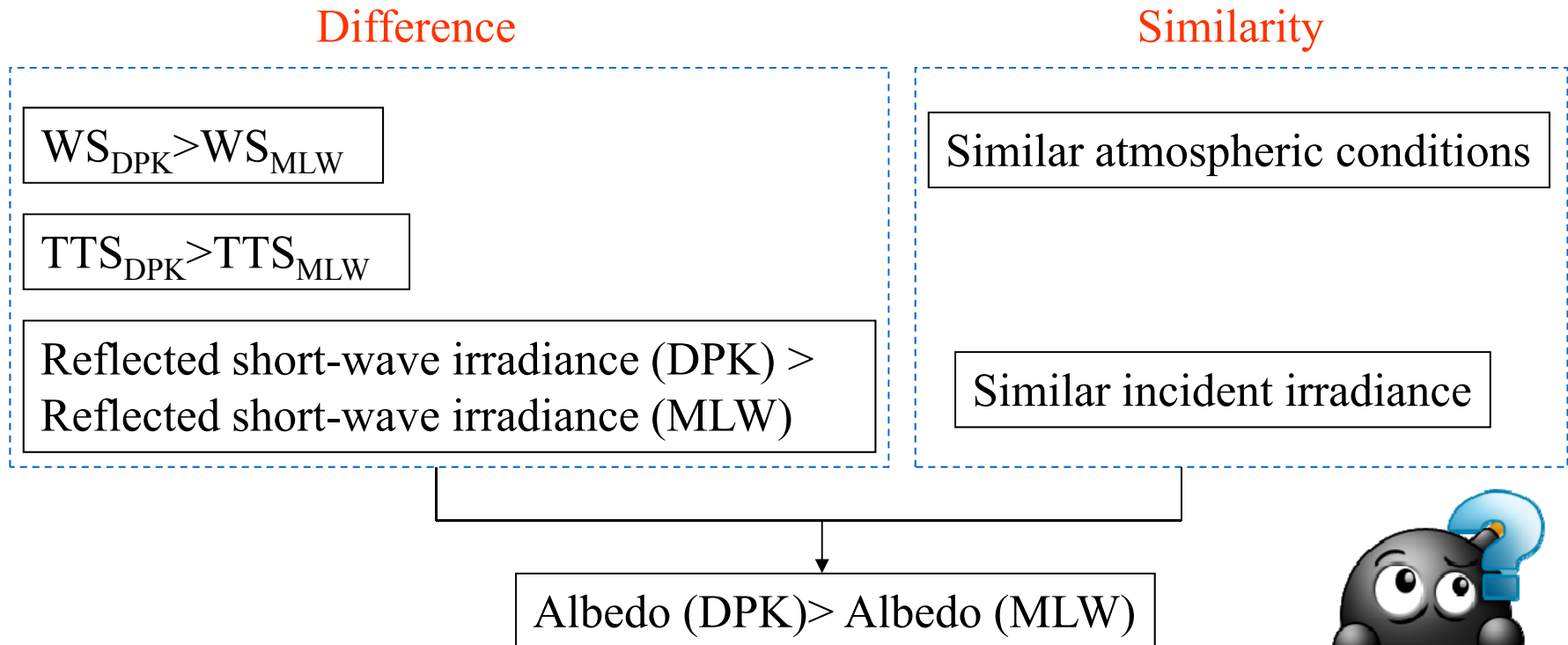
Main conclusions

- Modified SWIR-based atmospheric correction algorithm is suitable for highly turbid inland Lake Taihu;
- Algae usually appears in the **bay regions** (Meiliangwan Bay, Gonghu Bay and Zhushan Bay), and high Chl-a concentration were often observed during **late spring to early summer**;
- Waters in Taihu are consistently highly turbid all year around, TTS concentration, driven by wind is **high in winter-spring** seasons and **low in summer-fall** seasons;
- Inland freshwater optical and biological properties, as well as water quality can be monitored and evaluated quantitatively by RS measurements (MODIS).



4. Discussion

Hypothesis for daily mean water surface albedo analysis



The spatial pattern of daily mean albedo may be similar to TTS distribution pattern on local scale.

Difficulties for validation of lake color RS

- Reflection of bottom sediment in optical shallow regions;
- Asynchronism between RS measurement and in situ observation;
- Aerosol changing and fast variation of water color driven by wind;
- Spatial non-uniformity of water property in Lake Taihu.





Wang, 2011



南京信息工程大学
Nanjing University of Information Science & Technology

Look forward to your suggestions.

Thank you!



南京信息工程大学

Nanjing University of Information Science & Technology